In Vivo and Cytotoxicity Evaluation of Repaglinide-Loaded Binary Solid Lipid Nanoparticles After Oral Administration to Rats

MANOJ K. RAWAT, ACHINT JAIN, SANJAY SINGH

Department of Pharmaceutics, Institute of Technology, Banaras Hindu University, Varanasi 221005, Uttar Pradesh, India

Received 19 September 2010; revised 1 November 2010; accepted 2 December 2010

Published online 5 January 2011 in Wiley Online Library (wileyonlinelibrary.com). DOI 10.1002/jps.22454

ABSTRACT: The purpose of this work was to develop prolonged release binary lipid matrix-based solid lipid nanoparticles (SLN) of repaglinide (RG) for oral intestinal delivery and to improve the bioavailability of RG. SLN were designed by using glycerol monostearate and tristearin as lipid core materials and Pluronic-F68 as stabilizer. SLN were characterised by their particle size, zeta potential, entrapment efficiency, solid-state studies, *in vitro* drug release, particle surface and storage stability at 30°C/65% relative humidity for 3 months. Pharmacodynamic (PD) and pharmacokinetic (PK) studies were also performed in diabetes-induced rat. Moreover, an *in vitro* toxicity study was performed in rat macrophage cells to establish the safety of the prepared SLN. It was observed that binary lipid matrix-based SLN had better drug entrapment, desired release characteristics, spherical shape and maximum storage stability. Pharmacodynamic study indicated that RG delivered through binary SLN significantly reduces blood glucose, blood cholesterol and blood triglycerides level. The area under the curves after oral administration of optimised RG-SLN formulation and RG control were 113.36 ± 3.01 and 08.08 ± 1.98 h/(ng·mL), respectively. The relative bioavailability of RG was enhanced with optimised SLN formulation when compared with RG control. There was a direct correlation found between the plasma drug level (drug concentration) and the peak response (% blood glucose inhibition) in optimised RG-SLN batch. The *in vitro* toxicity study indicated that the SLN were well tolerated. © 2011 Wiley-Liss, Inc. and the American Pharmacists Association J Pharm Sci 100:2406–2417, 2011

Keywords: Repaglinide; solid lipid nanoparticles; lipid; crystal defects; first pass-metabolism; lymphatic transport; bioavailability; PK–PD correlation; lipid safety profile; cytotoxicity

INTRODUCTION

It is already estimated that the majority of the new drugs (approximately 60%) are poor water soluble.[1] Consequently, many of these substances have bioavailability problems after oral administration. To make these new drugs available to the patients, there is a definite need for smart oral formulations to enhance the bioavailability. Self-emulsifying delivery systems, liposomes, microemulsions, polymeric nanoparticles and recently solid lipid nanoparticles (SLN) have been exploited as probable carriers for oral intestinal lymphatic delivery. SLN were derived from oil-in-water emulsions by replacing the liquid lipid (oil) by a solid lipid, that is, a lipid being solid at room as well as at body temperature.[2,3] Because of their solid matrix, drug release from SLN can be modulated which could be used to optimise the plasma drug concentration profile.[4]SLN enhance lymphatic transport of the drugs, reduce the hepatic first-pass metabolism and improve bioavailability because intestinal lymph vessels drain directly into the thoracic duct, further into the venous blood, thus by passing the portal circulation.[5,6] Initially, Yang et al.[7] demonstrated the lymphatic uptake of camptothecin-loaded SLN after oral administration at preclinical level. Varshosaz et al.[8] and Hu et al.[9] reported that oral administration of buspirone HCL and digoxin-loaded SLN, respectively, improved the *in vitro* release as well as the oral bioavailability. Recently, Liu et al.[10] also studied the *in vitro* aspects of vitamin K_1 entrapped SLN after oral administration. A variety of matrix materials used for the fabrication of SLN are

Correspondence to: Sanjay Singh (Telephone: +91-542-670-2712; Fax: +91-542-23-68-428; E-mail: ssingh.phe@itbhu.ac.in, bitsmanoj@gmail.com)

Journal of Pharmaceutical Sciences, Vol. 100, 2406–2417 (2011)

hard fat or cetylpalmitate, fatty acid and glycerides (monoglycerides, diglycerides and triglycerides). SLN fabricated using lipids of less ordered crystal lattices favour successful drug inclusion compared with those prepared using highly ordered crystal lipids. This is owing to the crystallinity and polymorphic behaviour of lipids.[11] More complex lipids (triglycerides) form less perfect crystals with many imperfections. These imperfections offer space to accommodate the drug. Accordingly, crystallinity and polymorphic behaviour are the most essential key issues which have a strong influence on the drug incorporation and release rate. Therefore, degree of crystallinity is to be considered in selection of the lipids for formulation of SLN.

Single lipid matrix has perfect crystal lattice which is responsible for drug expulsion and consequently for less entrapment efficiency (EE) and physical instability.[12] On other side, binary lipid matrix can create deformation in crystal order of lipids and avoid the drug expulsion. Up to now, the use of binary lipid matrix in fabrication of SLN has not received due attention by the researchers. So as to improve the EE and physical stability of SLN, an attempt was made to disturb the crystal lattice (crystal order) of the monoglyceride [glycerol monostearate (GM)] by the addition of titrated trace amount of triglyceride [tristearin (TS)]. SLNs were loaded with an antidiabetic drug repaglinide (RG). The drug has low oral bioavailability with short terminal elimination half-life due to the first-pass metabolism.[13] With a view to improve the bioavailability, the drug-loaded binary SLN were prepared.

The prepared SLN were characterised for their particle size, polydispersity index (PDI), zeta potential, total drug content (TDC), EE, solid-state studies (differential scanning calorimeter), storage stability at 30°C/65% relative humidity (RH) for 3 months, *in vitro* drug release and particle surface studies (transmission electron microscopic analysis with electron diffraction (ED) pattern and atomic force microscopic analysis). The pharmacodynamic (PD) [blood glucose (BG), blood cholesterol (BC) and blood triglyceride (BT) level] and pharmacokinetic (PK) [AUC, T_{max}, C_{max}, K, $t_{1/2}$, mean residence time (MRT) and *%Fr*)] studies of selected formulation(s) were also carried out in diabetes-induced rats to investigate the oral bioavailability enhancement of RG-loaded SLN.

One can anticipate that SLN are well tolerated in living systems (mononuclear phagocytes) because they are made from physiological compounds and therefore, metabolic pathways exist. However, at frequent or higher dose, SLN can cause cytotoxicity by adherence of the particles to the cell membrane, degradation of the adherent nanoparticles and subsequent release of cytotoxic degradation products. Another mechanism is the internalisation of nanoparticles by cells, intracellular degradation and subsequent toxic effects inside the cell. Because of the phagocytic activity of the macrophage, both effects can potentially occur with the SLN.[14] Both immunomodulatory and cytotoxic effects of compritol and wax-prepared SLN on mononuclear phagocytes have been investigated by Scholer et al.[15] The concentration-dependent cytotoxicity of the SLN system was observed.[15,16] The cytotoxicity of SLN is determined by cell viability.

Therefore, apart from these characterisations, an *in vitro* toxicity study [MTT (3-(4,5-dimethylthiazol-2-yl)-2,5-diphenyl-tetrazolium bromide) assay] was also performed to evaluate the potential tolerability (cell viability) of RG-loaded SLN in rat macrophage cell.

MATERIALS AND METHODS

Samples of RG and GM were kind gifts from Wockhardt Research Centre (Aurangabad, Maharshtra, India). Tristearin was purchased from Sigma–Aldrich, Lyon, (France). Soya lecithin was purchased from Acros Organic, New Jersey (USA). Pluronic-F68 (PL-F68), sodium lauryl sulphate (SLS) and sodium carboxymethylcellulose (NaCMC) were generously supplied by SRL, Mumbai, (India). Dialysis membrane (molecular weight cut-off between 12,000 and 14,000 Da) was purchased from HiMedia, Mumbai, (India). All other chemicals were of analytical and high-performance liquid chromatography (HPLC) grade.

Preparation of SLN

Lipids and soya lecithin (0.04%, w/v) along with RG (0.02%, w/v) were dissolved in 2 mL of dichloromethane (DCM). Thereafter, the above mixture was immediately injected (1 mL/min) through an injection needle (0.45 mm/26 G) into the 100 mL aqueous phase containing 0.25 gm of PL-F68 under continuous stirring (2000 rpm for 2 h: Ika, Germany) at room temperature. Dichloromethane and some proportion of water were eliminated at 40°C under reduced pressure (Decibel, Digital Technologies, India), and the final volume of the aqueous nanosuspension was adjusted to 20 mL.

Repaglinide-loaded SLN obtained using GM and in combination with partial amount of TS (binary lipid matrix) were abbreviated as RGM (GM:TS 100:0), $RGMT_{10}$ (GM:TS 90:10), $RGMT_{20}$ (GM:TS 80:20) and $RGMT_{30}$ (GM:TS 70:30), respectively. Compositions of all the prepared formulations are shown in Table 1.

Particle Size and Zeta Potential Analysis

The particle size was measured by dynamic light scattering (Nano ZS, Malvern Instruments, Malvern, UK) and zeta potential was estimated on the basis of electrophoretic mobility under an electric field.

Table 1. SLN Composition for Different Preparations

Ingredients	RGM	$RGMT_{10}$	$RGMT_{20}$	$RGMT_{30}$
Repaglinide (mg)	20	20	20	20
Glycerol monostearate (mg)	200	180	160	140
Tristearin (mg)	–	20	40	60
Lecithin (mg)	40	40	40	40
Pluronic-F68 (mg)	250	250	250	250
Purified water (q.s. for 100 mL)				

High-performance liquid chromatography Analytical Method

HPLC analytical method was developed for the estimation of TDC, EE and *in vitro* drug release of RG-SLN. The analytical method was a reversed phase HPLC (Cecil CE4201, India) with an ultraviolet detector (282 nm). The HPLC column was Phenomenex (C18 reverse phase, 250 × 4.5 mm^2, 5 μ column). The mobile phase of acetonitrile–ammonium formate (pH 2.7; 0.01 mM) (60:40%, v/v) delivered with a flow rate of 1 mL/min. The retention time of the drug was found to be 4.51 ± 0.1 min.

Determination of total drug content (TDC)

Repaglinide-SLN nanosuspension (1 mL) were diluted to 10 mL with chloroform/ methanol mixture (1:2) and filtered by a 0.45-μm syringe filter (Millipore, Banglore, Karnataka. India), and TDC was determined by HPLC method as described above.

Determination of entrapment efficiency (EE)

The EE in nanosuspension was calculated as described by Muthu and Singh.[17] Free dissolved drug amount present in the nanosuspension was determined by bulk equilibrium reverse dialysis bag technique. Briefly, a dialysis bag (cellulose membrane, molecular weight cut-off 12,000–14,000 Da) containing 1 mL of distilled water with 25 mg PL-407 was placed directly into 10 mL of nanosuspension. After equilibrium (8 h), dialysis bag was withdrawn from the nanosuspension. Sample collected from dialysis bag was assayed by HPLC method as described above.

The calculation was performed as follows:

$$\text{Free dissolved drug} = \left(\frac{\text{Total volume}}{\text{Volume of dialysis bag}}\right) \times \text{Drug amount in the dialysis bag}$$

where total volume is the sum of total volume of the nanosuspension and volume of the dialysis bag sample.

$$\text{EE}\,(\%) = \left(\frac{\text{Total drug content} - \text{Free dissolved drug}}{\text{Drug amount used}}\right) \times 100$$

Solid-State Characterisation by DSC

Differential Scanning Calorimetry (DSC) thermograms of the different samples were obtained from a differential scanning calorimeter (DSC 30; Mettler–Toledo, Viroflay, France). Repaglinide, lipids and lyophilized RG-SLN were heated in sealed standard aluminum pans from 0°C to 160°C at a scanning rate of 10°C/min.

Stability Studies

To investigate the physical stability of the RG-SLN on storage, samples were stored for 3 months at 30°C/65% RH (Labtop stability chamber) and characterised with regards to particle size, PDI and EE.

In Vitro Release Study

In vitro release studies were performed using dialysis bag diffusion technique.[18–20] Dialysis membrane (molecular weight: 12,000 Da) was soaked in double-distilled water for 12 h before use for experiment. RG aqueous nanosuspension or RG control (RG suspension in 0.5% NaCMC) equivalent to 5 mg of RG were placed in the dialysis bag containing 50 mL of dissolution medium (phosphate buffer pH 6.8 containing 0.5% w/v SLS) at 37 ± 0.5°C with continuous magnetic stirring at 200 rpm. At fixed time intervals, the samples were withdrawn; same dissolution medium was replaced by fresh medium to maintain constant volume. Sink conditions were maintained for release studies ($C_1 < C_s \times 0.2$).[21]

C_1, final concentration of RG after the complete release of the drug in dissolution medium; C_s, saturation solubility of RG in the dissolution medium.

Samples were analysed by an HPLC method as described above.

Aqueous suspension of RG in 0.5% (w/v) NaCMC was used as RG control for the *in vitro* release studies.

Surface Structural Analysis

Surface Structural Analysis by Transmission Electron Microscope

The external morphology and ED pattern of SLN were determined by using transmission electron microscopy (TEM; TECNAI-12, FEI, Holland).

Surface Structural Analysis by Atomic Force Microscope

The surface properties of drug-loaded SLN were visualised by an atomic force microscope (AFM; Solver P-47-PRO, MDT, Moscow, Russia).

Animal Study Protocol

The study protocol was approved by the Animal Ethical Committee, Institute of Medical Science (Banaras Hindu University, Varanasi, Uttar Pradesh, India). Male wistar rats were obtained from Central animal laboratory (Varanasi). Rats had free access to food

(pellet diet supplied) and distilled water *ad libitum*. Thirty male rats weighing 170 ± 20 g were kept for overnight fasting with free access to water. Animals were divided into five groups comprising six animals in each group ($n = 6$). The animals of group I served as control, whereas group II served as diabetic control. All the animals of group III were given an oral dose of RG control, group IV was administered with RGM formulation orally and group V was given optimised batch of binary SLN in equivalent doses of RG orally.

Pharmacodynamic and Pharmacokinetic Study

Diabetes was induced in the rats using streptozotocin equivalent to 65 mg/kg body weight. Streptozotocin was dissolved in 0.5 mL of citrate buffer (pH 4.5) and administered intraperitoneally to the rats.[22] After 7 days, the extent of diabetic induction was monitored based on blood–sugar level. BG levels of at least 350 mg/dL were accepted as the basal level for diabetes. The rats were fasted for 18 h and the RG control (RG aqueous suspension in 0.5%, w/v NaCMC) or optimised batches of RG-SLN (0.286 mg/kg) were administered to the rats using gavage. Blood samples (0.5 mL) were collected from the retro-orbital vein in heparin-coated eppendorf tubes at 0.3, 1, 2, 4, 8, 16 and 24 h after drug administration.[23] The blood samples were centrifuged at 2347 × *g* (rpm: 5000 and r: 8.39 cm) for 5 min. Plasma was collected and stored at −40°C until analysis for BG, BC and BT levels.

Plasma Sample Preparation

Liquid-liquid extraction method was used for the determination of RG in human plasma. 1 ml RG solution (2, 4, 6, 8, 10 and 12 ng/ml) was added to blank plasma samples (150 µl) in centrifuge tube which is followed by further addition of 1 ml of extraction buffer (0.1M KH2PO4, pH 5.9). The mixture was vortexed, 5 mL of ethylacetate and 50 µL of isoamylalcohol were added and the pH was adjusted to 7.4 with 2M NaOH. The tubes were shaken manually for 10 min. This was followed by centrifugation at 2347 × *g* for 5 min. After centrifugation, the ethyl acetate phase was transferred into another centrifuge tubes and evaporated to dryness in vacuum oven on 400 mmHg pressure at 45°C. The dried extract was reconstituted with 40 µL of mobile phase.

Pharmacodynamic Analysis

The BG, BC and BT level were analysed by using glucose oxidase kit (GOD/POD method), cholesterol kit (Enzymatic CHOD-PAP method) and triglyceride liquid gold kit, respectively.[25] The areas under the effect curve versus time (AUEC) and Nadir effect are appropriate approaches for measuring the antidiabetic efficacy.[26] AUEC were determined from graphical plots of BG (% calculated based on the values for normal saline as the baseline) versus time (h). Nadir effect is the percent maximum lowering of glucose level at time t (t_{Nadir}) with respect to percentage of basal BG level.

Pharmacokinetic Analysis

Noncompartmental analysis with WinNonlin software (Version 4.1) was used to estimate the PK parameters ($C_{\max}$, $T_{\max}$, AUC, K, $t_{1/2}$ and MRT) of RG. Relative bioavailability (*%Fr*) of SLN formulations was calculated using the formula:

$$\%Fr = \left(\frac{\text{AUC}_{\text{SLN}}}{\text{AUC}_{\text{Suspension}}}\right) \times 100$$

Toxicological Study

Isolation of Rat Peritoneal Macrophage and Its Culture

Isolation of rat peritoneal macrophage was performed as described by Yassad et al.[27] Rats macrophages were isolated from their peritoneal fluid and suspended in a known volume of complete RPMI-1640 media supplemented with 10% fetal calf serum. Macrophages (1×10^5; 100 µL) were taken in each cavity of 96-well culture plates and incubated for 2 h at 37°C. After 2 h, culture supernatant was replaced with fresh complete media and these attached macrophages are used in the further following experiments.

MTT Assay

Cytotoxicity of RG-loaded SLN (RGM and RGMT_{30}) on rat macrophage cell was determined by the MTT assay.[28,29] MTT was dissolved in phosphate buffer saline at a concentration of 5.0 mg/mL. Twenty microlitres of the MTT solution was added into each 96-culture well containing 1×10^5 cells/100 µL after treatment with different doses (0.4, 0.6, 0.8, 1.0 and 1.2 mg/mL) of nanosuspension and RG control for 24 h and then incubated at 37°C for further 4 h. The plate was centrifuged for 5 min at 100 *g* at 4°C and the untransformed MTT was removed carefully by pipetting without disturbing the dark blue formazan (formed by cellular reduction of tetrazolium salt). To each well, 100 µL of a methanol was added and then placed on a plate shaker for 5 min at room temperature to dissolve the crystals of formazan and the optical density (OD) was evaluated in an ELISA reader (Labsystem, Multiscan) at a wavelength of 540 nm. Percent cell viability was expressed in percent compared with untreated cells (control). Each treatment was performed at least in triplicate wells, and the experiment was repeated for three times.

$$\%\ \text{Cell Viability} = \left(\frac{\text{OD}_{\text{SLN}}}{\text{OD}_{\text{Control}}}\right) \times 100$$

Statistical Analysis

The results were expressed as mean values ±SD. The analysis of variance (ANOVA) was applied to examine significance of differences between batches of nanoparticles properties. ANOVA followed by a *post hoc* Tukey multiple comparison test was performed for comparison in pharmacological evaluation of treatments. In all cases, $p < 0.05$ was considered to be significant.

RESULTS AND DISCUSSION

Measurement of Size, TDC and EE

SLN were prepared by modified solvent injection method. The lipids were dissolved in an organic solvent and rapidly injected into an aqueous phase containing the surfactant. This solvent injection technique relies on the rapid diffusion of the solvent across the solvent–lipid interface with the aqueous phase.[30,31] The mean particle size, PDI and zeta potential of RG-loaded SLN are shown in Table 2. PCS measurements were undertaken in multimodal analysis to get a factual reflection of particle size distribution. The particle size distribution curves for all the batches were unimodal.

Nanoparticle sizes and PDI ranged from 150 ± 3.04 to 325 ± 2.8 nm and 0.178 ± 0.022 to 0.280 ± 0.031, respectively for all the batches which indicate the narrow particle size distribution. The particle size of the RG-SLN was in the following order: $RGMT_{30}$ (150 ± 3.04) < $RGMT_{20}$ (192 ± 2.45) < $RGMT_{10}$ (240 ± 2.67) < RGM (325 ± 2.8). The increasing of TS content in SLN formulations could reduce the melting point of GM lipid matrix and crystal order disturbance in lipid matrix, leading to favour the formation of SLN with smaller particle size. Zeta potential is an important factor to evaluate the stability of colloidal suspension.[17] The zeta potential of the studied formulations varied from -24.10 ± 2.71 to -25.98 ± 1.69 mV which is nearer to −25 mV of ideal stabilisation.[32] No significant ($p > 0.05$) difference in the zeta potential of SLN was observed in case of all formulations. In all prepared batches, TDC (assay) was nearer to 98%. The EE of the RG-SLN was in the order of RGM (59.13 ± 2.17) < $RGMT_{10}$ (65.14 ± 2.35) < $RGMT_{20}$ (77.14 ± 1.95) < $RGMT_{30}$ (87.40 ± 2.84). Single lipid-based SLN have shown significantly lesser drug EE than binary lipid-based SLN ($p < 0.05$). The higher EE with the binary lipid matrix-based SLN ($RGMT_{30}$) is attributed to the deformation of the crystal lattice of the GM lipid by TS lipid as well as increase the solubility of RG in lipid matrix.[33] By adding the TS to the GM carrier, the EE is increased in a concentration-dependent manner. EE of the drug in the lipids depends upon the factors such as miscibility, solubility of drug in lipid melt, physical and chemical structure of the lipid matrix and crystalline state of lipid materials.[11]

Solid-State Characterisation

Differential scanning calorimetry gives an insight into the melting and recrystallisation behaviour of crystalline material like SLN. The breakdown of the crystal lattice by heating the sample gives detail information on, for example, polymorphism, crystal ordering, eutectic mixtures or glass transition processes.[34] Differential scanning calorimetry experiments are useful to understand solid dispersions such as solid solutions, simple eutectic mixtures or, as in this case, effect of TS lipid on crystal ordering of GM lipid. Figures 1a–1g give an overview of the melting process of a RG-SLN. The SLN were formulated with different ratios of GM to TS lipids combination (GM: TS 100:0, 90:10, 80:20 and 70:30). Figure 1d represents GM made SLN (RGM) by using the modified solvent injection technique containing 0.2%, (w/v) GM (GM:TS ::100:0). The Figures 1e–1g were recorded on lipid carriers with increasing TS amounts ($RGMT_{10}$, $RGMT_{20}$ and $RGMT_{30}$). For the RGM, the melting process takes place with maximum temperature at 57.02°C (peak maximum). By adding the TS to the GM carrier, the melting point is depressed in a concentration-dependent manner. At 90:10, 80:20 and 70:30 GM: TS lipid ratios, the melting points are depressed in following manners, 53.18°C, 48.03°C and 44.03°C, respectively. Such a phenomenon was attributed to the small size of the nanoparticles and their high specific surface area which can reduce their melting point by several degrees.[35] Apart from this, the presence of guest molecules in the lipid matrix also influences its crystallisation degree and the lipid layer organisation.[36]

Table 2. SLN Characteristics for Different Preparations (Mean Values ± SD; $n = 3$)

Batch Code	Particle Size (nm)	PDI	Zeta Potential (mV)	TDC (%)	EE (%)
RGM	325 ± 2.8	0.280 ± 0.031	-24.10 ± 2.71	99.78 ± 2.06	59.13 ± 2.17
$RGMT_{10}$	240 ± 2.67	0.210 ± 0.091	-24.85 ± 2.29	99.46 ± 1.98	65.14 ± 2.35
$RGMT_{20}$	192 ± 2.45	0.196 ± 0.042	-25.03 ± 2.38	98.89 ± 2.22	77.14 ± 1.95
$RGMT_{30}$	150 ± 3.04	0.178 ± 0.022	-25.98 ± 1.69	98.39 ± 2.16	87.40 ± 2.84

SLN, solid lipid nanoparticle; PDI, polydispersity index; TDC, total drug content; EE, entrapment efficiency.

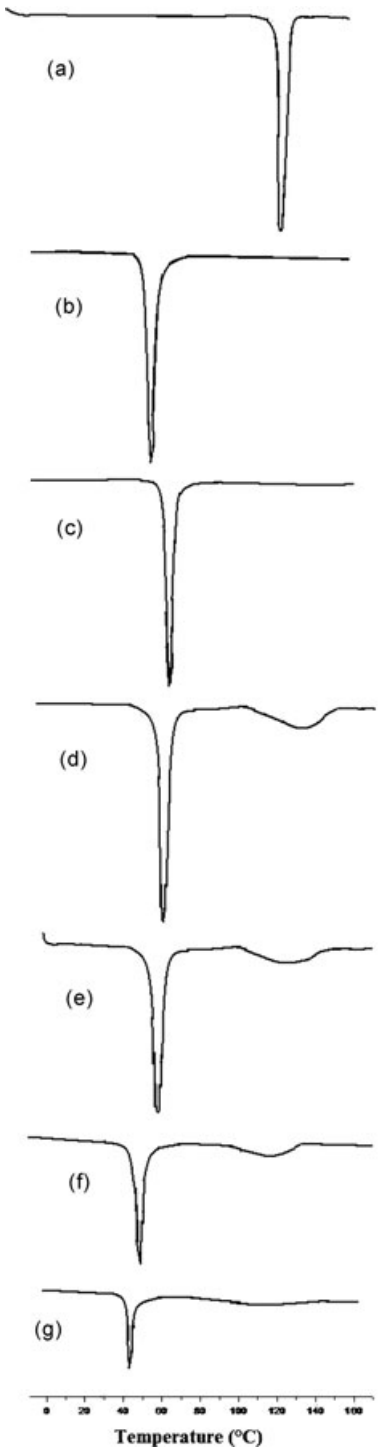

Figure 1. Differential scanning calorimetry thermograms: (a) repaglinide, (b) glycerol monostearate, (c) tristearin, (d) RGM, (e) $RGMT_{10}$, (f) $RGMT_{20}$ and (g) $RGMT_{30}$.

Stability Studies

In all SLN batches, storage at 30°C/65% RH for 3 months resulted in increase in particle size as well as PDI. Increase in particle size was in the following manner: RGM (358 ± 2.9 nm) >$RGMT_{10}$ (291 ± 3.06 nm) >$RGMT_{20}$ (204.6 ± 1.98 nm) >$RGMT_{30}$ (154 ± 2.34 nm). However, SLN prepared with $RGMT_{30}$ did not show any statistically significant increase in particle size ($p > 0.05$). SLN prepared with binary lipid matrix ($RGMT_{30}$) exhibited greater storage stability, whereas SLN with GM alone showed increase in particle size and particle agglomeration (increase in PDI). A significant increase in PDI was observed in all batches except $RGMT_{30}$ (Table 3). The decrease in EE of all the batches was in following order: 20.09% (RGM) >9.23% ($RGMT_{10}$) >7.54% ($RGMT_{20}$) >5.03% ($RGMT_{30}$) after storage. However, the decrease was too low in $RGMT_{30}$ batch which virtually indicates the stability of SLN. The degree of crystallinity and presence of 50% of monoglycerides in glycerylmonostearate (GM) are responsible for the physical destabilisation leading to drug expulsion.[35] Because of this, EE was found to decrease on storage. The higher ratio of TS in the GM lipid was responsible for better stability of $RGMT_{30}$. The presence of TS in GM prepared nanoparticles disturbs the crystalline order, and this causes delay in recrystallisation and thus improves physical stability.

Saturation Solubility and *In Vitro* Release Studies

The saturation solubility (C_s) of RG in phosphate buffer pH 6.8 containing 0.5% SLS was 610.5 μg/mL at 37 ± 0.5°C. Sink conditions were maintained for release study: $C_1 < C_s \times 0.2$.[21] C_1 was the final concentration of RG in medium after complete release of the drug in the phosphate buffer pH 6.8 containing 0.5% SLS. Therefore, the final concentration of RG after the complete release in dissolution media was maintained below 122.1 μg/mL, in compliance with the sink conditions.

The release rate of the RG from the SLN and its appearance in the dissolution medium was governed by the partition coefficient of the drug between the lipid phase and the aqueous environment in the dialysis bag and by the diffusion of the drug across the membrane as well. Dialysis bag retained nanoparticles and allowed the diffusion of the drug immediately into the receiver compartment. Figure 2 shows the cumulative percent release of RG from RG control, RGM and $RGMT_{30}$ batches. Complete RG release (100%) was achieved within 8 h from the RG control across the dialysis bag which indicates rapid diffusion of the RG. In case of the RG control, the time required for 50% drug release ($T_{50\%}$) was 1.5 ± 0.01 h, whereas $T_{50\%}$ for different batches of SLN were: RGM (2.30 ± 0.025 h), $RGMT_{10}$ (3.1 ± 0.05 h), $RGMT_{20}$ (3.32 ± 0.027 h) and $RGMT_{30}$ (4.05 ± 0.04 h). The prolonged drug release was observed in $RGMT_{30}$ batches as compared with RGM. This is probably caused by the high lipophilicity of binary lipid matrix compared with single lipid matrix (RGM) due to more carbon chains contributing to the more prolong release effect.

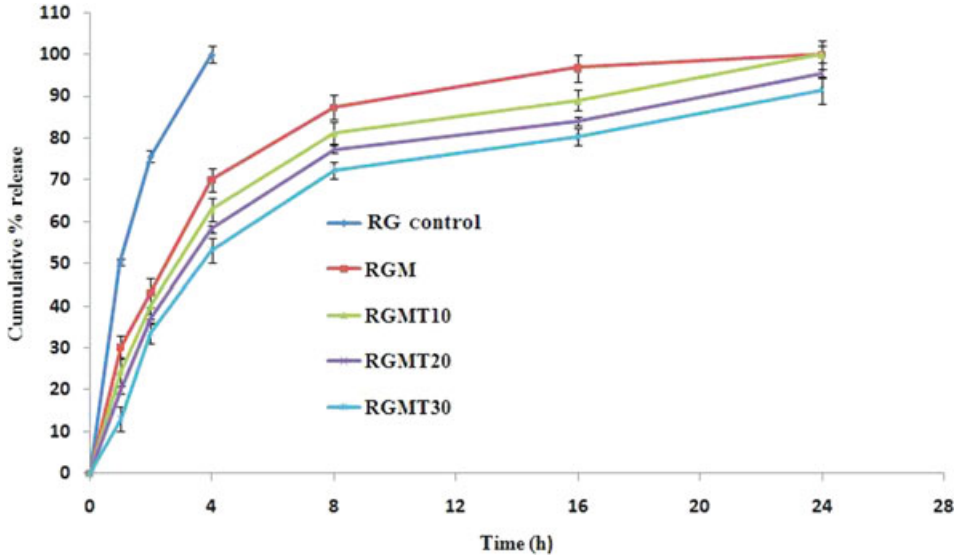

Figure 2. *In vitro* drug release from repaglinide (RG) suspension and RG-SLN batches. SLN, solid lipid nanoparticles.

The prolonged release characteristics of nanoparticles coupled to the steric repulsion properties could be a beneficial delivery system as long circulating carriers in drug delivery applications.[37] $RGMT_{30}$ has shown small particle size, high EE, best physical stability and prolonged release. Therefore, from binary lipid matrix-based SLN, $RGMT_{30}$ batch has been selected for further studies.

Surface Structural Analysis

The external morphological study using TEM revealed that placebos SLN as well as drug SLNs were spherical in shape (Figures 3a and 3b). The shape of SLN is guided by the properties of lipid (including solubility) and its crystal lattice.[38] The SLN size, as observed by TEM, correlated well with the size measured by Malvern zetasizer.

Electron diffraction of the drug loaded ($RGMT_{30}$) and placebo (without drug) SLN in TEM revealed the crystalline state of the SLN (Figures 4a and 4b). These images clearly demonstrate that ring patterns in the ED were reduced in drug-loaded SLN owing to presence of amorphous RG.[20] This study confirmed that RG was well incorporated into the core of SLN (Figure 4b). The presence of amorphous RG was also revealed in DSC study.

Multi-nanoparticles and three-dimensional (3D) AFM images of $RGMT_{30}$ in Figures 5a and 5b, respectively, showed smooth nanoparticle surface without any noticeable pinholes or cracks. AFM also revealed that all SLNs were spherical in shape and around 150 nm in size. The SLN size as observed by AFM correlated well with the size measured by PCS. Further, the average roughness (Sa) of nanoparticles were 6.0378 nm which also indicates the surface smoothness of SLN (3D image).

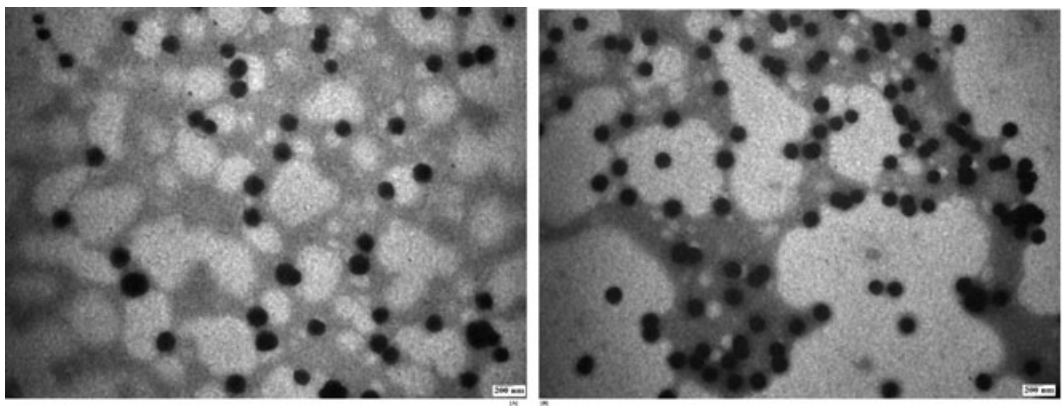

Figure 3. Transmission electron micrographs of Placebo solid lipid nanoparticles and $RGMT_{30}$.

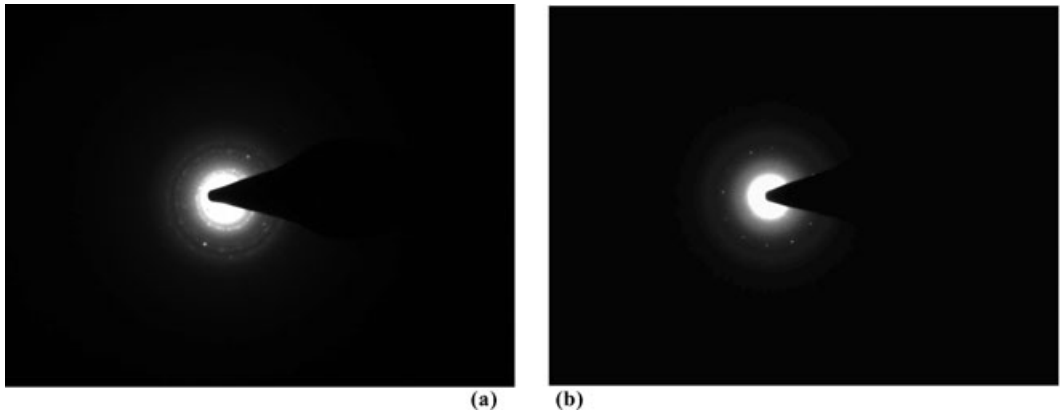

Figure 4. Electron diffraction ring pattern for placebo solid lipid nanoparticles and $RGMT_{30}$.

Pharmacodynamic and Pharmacokinetic Studies

Figures 6a–6c show the BG, BC and BT levels, respectively, at different time intervals following oral administration of RG-SLN (RGM and $RGMT_{30}$) and RG control at a dose of 0.286 mg/kg to diabetic rats. From Figures 6a–6c, it is clear that the administration of RG-SLN had a significant influence on BG, BC and BT level compared with RG control ($p < 0.05$). In streptozotocin-induced diabetic rats, the maximal effect was registered 0.3 h after treatment with the RG control and 4 h after treatment with RG-SLN. The AUEC obtained for RGM and $RGMT_{30}$ were 1324.59 $\pm$ 3.43% and 1524.69 $\pm$ 3.12% h, respectively, whereas 49.41 $\pm$ 2.86% h for RG control (Table 4). The $RGMT_{30}$ and RGM showed a greater antidiabetic effect for longer period of time (in terms of basal reduction in BG level) than RG alone. This clearly indicates that lipid concentration in formulation is sufficient to prolong the drug release for longer period of time. After the oral administration, the t_{Nadir} for RG control was 0.3 h and for RGM and $RGMT_{30}$ batches, it was 4 h (Table 4). The Nadir effect for RG control, RGM and $RGMT_{30}$ were 62.52 $\pm$ 2.55, 61.855 $\pm$ 1.78 and 69.00 $\pm$ 1.06, respectively. Figures 6b and 6c clearly indicate that the administration of RG-SLN had a significant influence on blood lipid levels (BC and BT) compared with RG control and able to reduce the blood lipid profiles for prolong period of time in diabetes-induced rats ($p < 0.05$). This again clearly indicates that RG-SLN were more effective than RG in lowering of glucose levels and also in sustaining the drug release for longer period of time. Although the developed RG-SLN had shown better *in vitro* dissolution and PD behaviour, the formulations RGM and $RGMT_{30}$ were also evaluated for its oral bioavailability in diabetic rats to ascertain the PK parameters (AUC, T_{max}, C_{max}, K, $t_{1/2}$, MRT and % Fr).

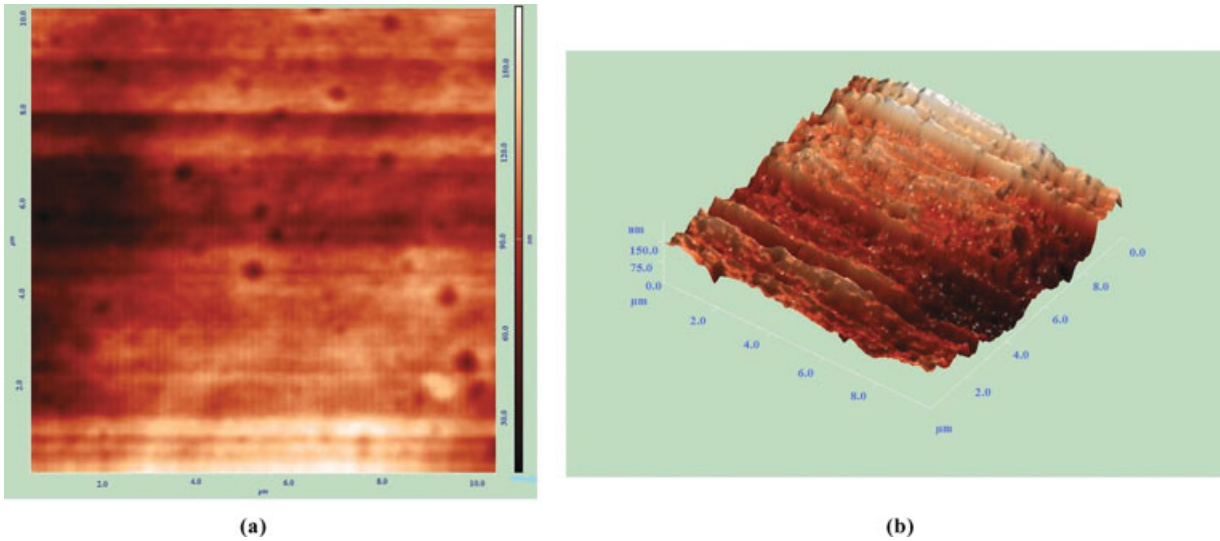

Figure 5. **(a)** AFM image (multi-nanoparticles), **(b)** AFM image (three dimensional) of $RGMT_{30}$ batch.

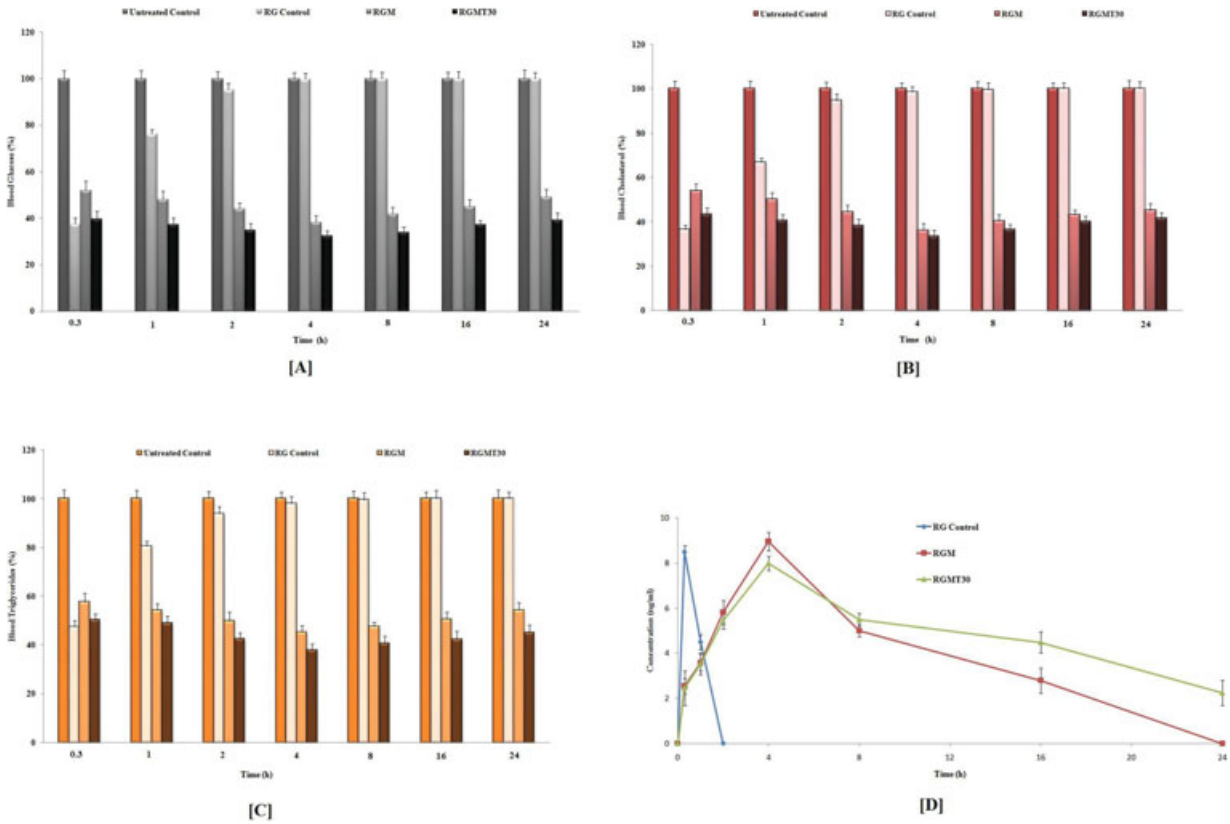

Figure 6. (a) Blood glucose, (b) cholesterol, (c) triglycerides and (d) mean plasma time–concentration curves after administration of repaglinide (RG) suspension and RG-SLN (mean ± SD; $n = 6$).

Plasma concentration–time curve of RG and RG-SLN after oral administration are shown in Figure 6d. Peak plasma concentrations (C_{max}) for RG control, RGM and $RGMT_{30}$ were 8.50 ± 0.01, 8.97 ± 0.045 and 8.01 ± 0.089 ng/mL, respectively. T_{max} values were same (4.00 h) for RGM and $RGMT_{30}$, but for RG control, it was 0.3 h (Table 5). The AUCs of the SLN [RGM: 97.04 ± 2.01 and $RGMT_{30}$: 113.36 ± 3.01 h/(ng mL.) were significantly ($p < 0.05$) higher than that of RG control [8.08 ± 1.98 h/(ng mL). Relative bioavailabilities (*%Fr*) were in the following order: $RGMT_{30}$ (1402.970 ± 3.03) >RGM (1200.99 ± 2.56) >RG control (100). Increase in AUC and *%Fr* for SLNs indicate that RG oral absorption was enhanced significantly compared with the RG control. Mean residence time of $RGMT_{30}$ was also increased significantly ($p < 0.05$) when compared with RGM and RG control (Table 5). This may be attributed to the presence of long-chain fatty acid (TS) along with GM in $RGMT_{30}$. The long $t_{1/2}$ and higher MRT of $RGMT_{30}$ as compared with RGM and RG control (Table 5) indicate the prolonged release properties of $RGMT_{30}$ formulation. Increase in AUC and *%Fr* for SLN might be due to the avoidance of first-pass metabolism by lymphatic transport because poor bioavailability of RG was mainly due to the first-pass metabolism.[39,40] Lipid nature, fatty acid chain length and hydrophobicity will influence the lymphatic uptake.[41–43] Esterification of long-chain fatty acids (TS) formed surface-active monoacylgycerol and diacylgycerol which can solubilise RG and subsequently, interaction with bile salts takes place, leading to the formation of mixed micelles which promote RG absorption though lymphatic route.[44] The EE, physical stability, *in vitro*

Table 3. Stability Studies for Different SLN Formulation at Storage Condition 30°C/65% RH for 3 Months (Mean Values ± SD; $n = 3$)

Parameters	RGM	$RGMT_{10}$	$RGMT_{20}$	$RGMT_{30}$
Particle size (nm)	358 ± 2.9	291 ± 3.06	204.6 ± 1.98	153.02 ± 2.34
PDI	0.420 ± 0.020	0.301 ± 0.041	0.254 ± 0.033	0.188 ± 0.052
EE (%)	47.25 ± 2.42	59.13 ± 2.51	71.32 ± 1.98	83.0 ± 2.31

SLN, solid lipid nanoparticle; RH, relative humidity; PDI, polydispersity index; EE, entrapment efficiency.

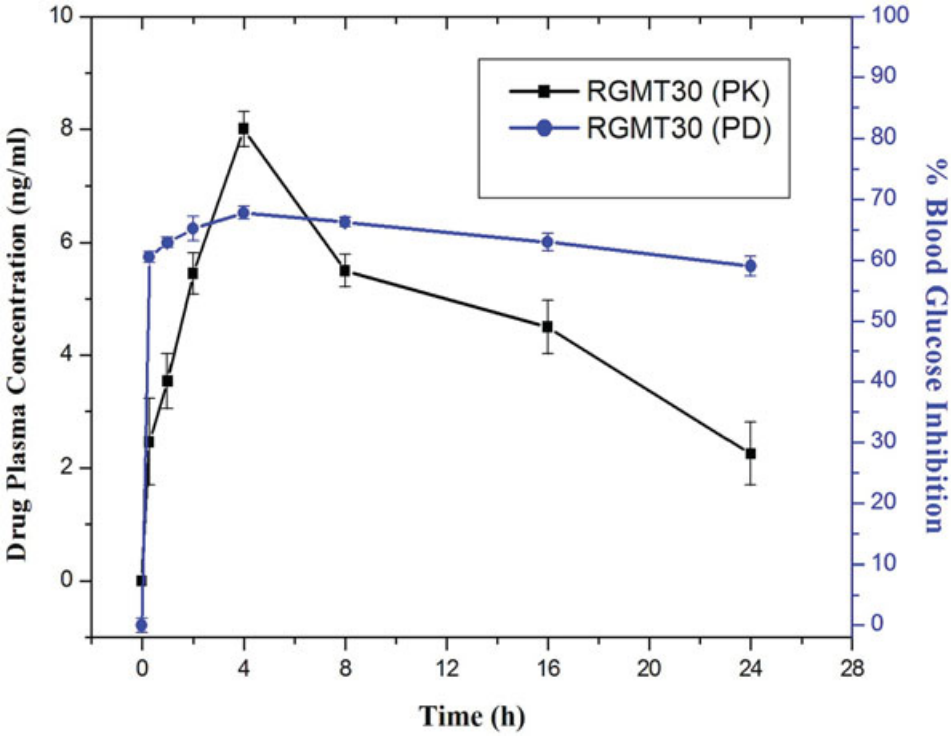

Figure 7. PK–PD study of $RGMT_{30}$ batch.

drug release and *in vivo* results indicate that $RGMT_{30}$ batch is the best among the different batches of RG-SLN.

It is observed from the PD and PK properties for the $RGMT_{30}$ batch that there was a direct correlation between the plasma drug level (drug concentration) and the peak response (% BG inhibition). Figure 7 indicates that as the RG plasma level reduces, the BG lowering effects of RG also decreases simultaneously but not in similar fashion. Time to attain peak plasma concentration (T_{max}) and peak response are same. So, there is no lag period between peak plasma concentration (C_{max}) and peak response. Thus, PK–PD profile of RG is well correlated.

Furthermore, the *in vitro* toxicity (% cell viability) of the optimised batch ($RGMT_{30}$) and RG control was evaluated as described in the aforementioned method. The OD of $RGMT_{30}$ batch was not significantly different from control (untreated cells), indicating no change in the number of viable cells ($p > 0.05$). Cells were proliferated normally till 24 h as evident by the MTT assay (Figure 8). This result suggests that the fabricated SLNs were well tolerated and do not form any toxic leachable or degradation products and thus can be used for drug delivery applications.

Finally, it can be established from the above study that SLN enhanced the oral bioavailability of RG. Moreover, SLN developed from binary lipid matrix showed more promising *in vitro* and *in vivo* results than single lipid core materials and thus may be used as a suitable carrier system for oral delivery of RG.

Table 4. Pharmacodynamic Studies of the Repaglinide Formulations

Preparation	AUEC (% h)	Nadir Effect (%)	t_{Nadir} (h)
RG control	49.41 ± 2.86	62.52 ± 2.55	0.3 ± 0.06
RGM	1324.59 ± 3.43*	61.855 ± 1.78	4 ± 0.083*
$RGMT_{30}$	1524.69 ± 3.12†*	69.00 ± 1.06†*	4 ± 0.078*

*Statistical significance with RG control, $p < 0.05$.
†Statistical significance with RGM, $p < 0.05$.
AUEC, areas under the effect curve versus time; RG, repaglinide.

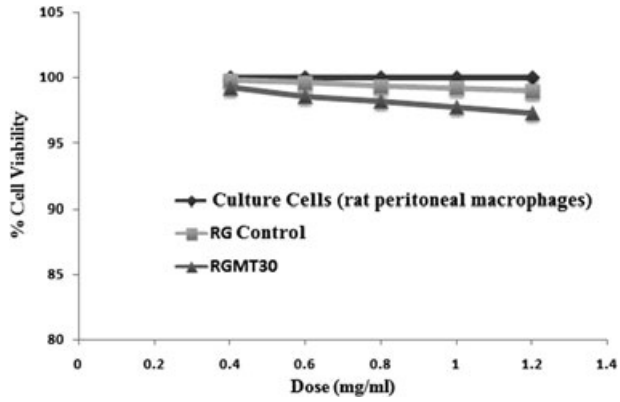

Figure 8. *In vitro* toxicity analysis (MTT assay) of repaglinide (RG) suspension and RG-SLN (mean ± SD; $n = 6$).

Table 5. Pharmacokinetic Studies of the Repaglinide Formulations

Parameters	RG Control	RGM	$RGMT_{30}$
T_{max} (h)	0.300 ± 0.03	4.00 ± 0.071*	4.00 ± 0.082*
C_{max} (ng/mL)	8.50 ± 0.01	8.97 ± 0.045	8.01 ± 0.089
K (h^{-1})	0.66 ± 0.040	0.08 ± 0.09*	0.058 ± 0.098†*
$t_{1/2}$ (h)	1.05 ± 0.24	8.44 ± 0.61*	11.98 ± 0.230†*
AUC [h/(ng·mL)]	8.08 ± 1.98	97.04 ± 2.01*	113.36 ± 3.01†*
MRT (h)	1.52 ± 0.67	12.18 ± 0.07*	17.29 ± 0.10†*
%Fr	100	1200.99 ± 2.56*	1402.970 ± 3.03†*

*Statistical significance with RG control, $p < 0.05$.
†Statistical significance with RGM, $p < 0.05$.
RG, repaglinide; AUC, area under the curves; MRT, mean residence time.

CONCLUSION

The present study confirms that the modified solvent injection is a suitable technique for the preparation of RG-SLN. The binary lipid matrix resulted in high EE. The DSC, TEM, ED ring pattern and AFM analysis showed the amorphous state of RG in SLN. The stability data and *in vitro* release profile indicated controlled release of the drug and excellent physical long-term stability in binary lipid-based SLN. SLN developed from binary lipid matrix showed more promising PD and PK results than single lipid core materials. Furthermore, *in vitro* toxicity study showed that the prepared SLN were well tolerated. The current investigation opens new prospect of successful utilisation of binary lipid matrix as a carrier for delivery of lipophilic drug(s).

ACKNOWLEDGMENTS

We acknowledge the help of Dr. Rajeev Prakash, Department of Material Science & Technology and Prof. G. Singh and Dr. Madhu Yashpal, Department of Anatomy, Institute of Medical Sciences, Banaras Hindu University, Varanasi, India in carrying DSC & AFM and TEM analysis of solid lipid nanoparticles nanoparticles, respectively. We also acknowledge the University Grant Commission (UGC), India for providing the financial support in the form of the Senior Research Fellowship.

REFERENCES

1. Fahr A, Liu X. 2007. Drug delivery strategies for poorly water-soluble drugs. Expert Opin Drug Deliv 4:403–416.
2. Muller RH, Mehnert W, Lucks JS, Schwarz C, Muhlen AZ, Weyhers H, Freitas C, Ruhl D. 1995. Solid lipid nanoparticles (SLN)-an alternative colloidal carrier system for controlled drug delivery. Eur J Pharm Biopharm 41:62–69.
3. Muller RH, Mader K, Gohla S. 2000. Solid lipid nanoparticles (SLN) for controlled drug delivery-a review of the state of art. Eur J Pharm Biopharm 50:161–177.
4. Muhlen AZ, Schwarz C, Mehnert W. 1998. Solid lipid nanoparticles (SLN) for controlled drug delivery-drug release and release mechanism. Eur J Pharm Biopharm 45:149–155.
5. Porter CJ, Charman WN. 2001. *In vitro* assessment of oral lipid based formulations. Adv Drug Deliv Rev 50:S127–S147.
6. Cai Z, Wang Y, Zhu LJ, Liu ZQ. 2010. Nanocarriers: A general strategy for enhancement of oral bioavailability of poorly absorbed or pre-systemically metabolized drugs. Curr Drug Metab 11:197–207.
7. Yang S, Zhu J, Lu Y, Liang B, Yang C. 1999. Body distribution of camptothecin solid lipid nanoparticles after oral administration. Pharm Res 16:751–757.
8. Varshosaz J, Tabbakhian M, Mohammadi MY. 2009. Formulation and optimization of solid lipid nanoparticles of buspirone HCl for enhancement of its oral bioavailability. J Liposome Res 3:1–11.
9. Hu L, Jia H, Luo Z, Liu C, Xing Q. 2010. Improvement of digoxin oral absorption in rabbits by incorporation into solid lipid nanoparticles. Pharmazie 65:110–113.
10. Liu CH, Wu CT, Fang JY. 2010. Characterization and formulation optimization of solid lipid nanoparticles in vitamin K1 delivery. Drug Dev Ind Pharm 6:1–11.
11. Manjunath K, Reddy JS, Venkateswarlu V. 2005. Solid lipid nanoparticles as drug delivery systems. Methods Find Exp Clin Pharmacol 27:127–144.
12. Mehnert W, Mader K. 2001. Solid lipid nanoparticles: Production, characterization and applications. Adv Drug Deliv Rev 47:165–196.
13. Mayer-Davis EJ, Levin S, Bergman RN. 2001. Insulin secretion, obesity, and potential behavioral influences: Results from the Insulin Resistance Atherosclerosis Study (IRAS). Diabetes Metab Res 17:137–145.
14. Muller RH, Massen S, Schwarz C, Mehnert W. 1997. Solid lipid nanoparticles (SLN) as potential carrier for human use: Interaction with human granulocytes. J Control Rel 47:261–269.
15. Scholer N, Zimmermann E, Katzfey U, Hahn H, Muller RH, Liesenfeld O. 2000. Effect of solid lipid nanoparticles (SLN) on cytokine production and the viability of murine peritoneal macrophages. J Microencapsul 17:639–650.
16. Scholer N, Hahn H, Muller RH, Liesenfeld O. 2002. Effect of lipid matrix and size of solid lipid nanoparticles (SLN) on the viability and cytokine production of macrophages. Int J Pharm 14:167–176.
17. Muthu MS, Singh S. 2008. Studies on biodegradable polymeric nanoparticles of risperidone: *In vitro* and *in vivo* evaluation. Nanomedicine 2:233–240.
18. Verger ML, Fluckiger L, Kim Y. 1998. Preparation and characterization of nanoparticles containing an antihypertensive agent. Eur J Pharm Biopharm 46:137–143.
19. Holm R, Mullertz A, Christensen E, Hoy CE. 2001. Comparison of total oral bioavailability and the lymphatic transport of halofantrine from three different unsaturated triglycerides in lymph-cannulated conscious rats. Eur J Pharm Sci 14:331–337.
20. Singh S, Muthu MS. 2007. Preparation and characterization of nanoparticles containing an atypical antipsychotic agent. Nanomedicine 3:305–319.

21. Moneghini M, Volinovich D, Princivalle F. 2000. Formulation and evaluation of vinypyrrolidone/vinylacetate copolymer microspheres with carbamazepine. Pharm Dev Technol 5:347–353.
22. Kim A, Yun MO, Oh YK, Ahn WS, Kim CK. 1999. Pharmacodynamic of insulin in polyethylene glycol-coated liposomes. Int J Pharm 180:75–81.
23. Lu Y, Zhang Y, Yang Z, Tang X. 2009. Formulation of an intravenous emulsion loaded with clarithromycin-phospholipid complex and its pharmacokinetics in rats. Int J Pharm 366:160–169.
24. Ruzilawati AB, Wahab MSA, Imran A, Ismail Z, Gana SH. 2007. Method development and validation of repaglinide in human plasma by HPLC and its application in pharmacokinetic studies. J Pharm Biomed Anal 43:1831–1831.
25. Goldberg IJ, Isaacsa A, Sehayekb E, Breslowb JL, Huanga LS. 2004. Effects of streptozotocin-induced diabetes in apolipoprotein AI deficient mice. Atherosclerosis 172:47–53.
26. Adikwu MU, Yoshikawa Y, Takada K. 2004. Pharmacodynamic-pharmacokinetic profiles of metformin hydrochloride from a mucoadhesive formulation of a polysaccharide with antidiabetic property in streptozotocin-induced diabetic rat models. Biomaterials 25:3041–3048.
27. Yassad A, Lavoinne A, Bion A, Daveau M, Husson A. 1997. Glutamine accelerates interleukin-6 production by rat peritoneal macrophages in culture. FEBS Lett 413:81–84.
28. Mosmann T. 1983. Rapid colorimetric assay for cellular growth and survival: Application to proliferation and cytotoxicity assays. J Immunol Methods 65:55–63.
29. Grando FC, Felicio CA, Twardowschy A, Paula FM, Batista VG, Fernandes LC, Curi R, Nishiyama A. 2009. Modulation of peritoneal macrophage activity by the saturation state of the fatty acid moiety of phosphatidylcholine. Braz J Med Biol Res 42:599–605.
30. Quintanar GD, Allemann, E, Doelker E, Fessi H. 1997. A mechanistic study of the formation of polymer nanoparticles by the emulsification-diffusion technique. Colloid Polymer Sci 275:640–647.
31. Schubert MA, Muller-Goymann CC. 2003. Solvent injection as a new approach for manufacturing lipid nanoparticles. Evaluation of the method and process parameters. Eur J Pharm Biopharm 55:125–131.
32. Betancourt T, Brown B, Brannon-Peppas L. 2007. Doxorubicin—loaded PLGA nanoparticles by nanoprecipitation: Preparation, characterization and in vitro evaluation. Nanomedicine 2:219–232.
33. Jenning V, Thunemann AF, Gohla SH. 2000. Characterisation of a novel solid lipid nanoparticle carrier system based on binary mixtures of liquid and solid lipids. Int J Pharm 199:167–177.
34. Bunjes H, Westesen K, Koch MHJ. 1996. Crystallization tendency and polymorphic transitions in triglyceride nanoparticles. Int J Pharm 129:159–173.
35. Jenning V, Gohla SH. 2001. Encapsulation of retinoids in solid lipid nanoparticles (SLN). J Microencapsul 18:149–158.
36. Westesen K, Bunjes H, Koch MHJ. 1997. Physicochemical characterization of lipid nanoparticles and evaluation of their drug loading capacity and sustained release potential. J Control Release 48:223–236.
37. Reddy H, Murthy RSR. 2005. Etoposide-loaded nanoparticles made from glyceride lipids: Formulation, characterization, in vitro drug release, and stability evaluation. AAPS PharmSciTech 6:E158–E166.
38. Hu FQ, Jiang SP, Du YZ. 2005. Preparation and characterization of stearic acid nanostructured lipid carriers by solvent diffusion method in an aqueous system. Colloids Surf B Biointerfaces 45:167–173.
39. Mansbach CM, Nevin P. 1998. Intracellular movement of triacylglycerols in intestine. J Lipid Res 39:963–968.
40. Cavalli R, Bargoni A, Podio V, Muntoni E. 2003. Duodenal administration of solid lipid nanoparticles loaded with different percentages of tobramycin. J Pharm Sci 92:1085–1094.
41. Ros E. 2000. Intestinal absorption of triglyceride and cholesterol, dietary and pharmacological inhibition to reduce cardiovascular risk. Atherosclerosis 151:357–379.
42. Nordskog BK, Phan CT, Nutting DF, Tso P. 2001. An examination of the factors affecting intestinal lymphatic transport of dietary lipids. Adv Drug Deliv Rev 50:21–44.
43. Holm R, Mullertz A, Pedersen GP, Christensen HG. 2001. Comparison of the lymphatic transport of halofantrine administered in disperse systems containing three different unsaturated fatty acids. Pharm Res 18:1299–1304.
44. Muller RH, Runge S, Ravelli V, Mehnert W, Thunemann AF, Souto EB. 2006. Oral bioavailability of cyclosporine: Solid lipid nanoparticles (SLN) versus drug nanocrystals. Int J Pharm 317:82–89.